Backward- and traveling-wave tubes with dielectric-lined rippled-wall waveguides

Bao-Liang Qian, Chuan-Lu Li, and Yong-Gui Liu
Department of Applied Physics, Changsha Institute of Technology, Changsha 410073, Hunan, People's Republic of China
(Received 24 April 1995; revised manuscript received 28 September 1995)

This paper presents the concept of a dielectric backward-wave tube or a dielectric traveling-wave tube, in which the relativistic electron beam guided by a strong magnetic field propagates through a dielectric-lined cylindrical waveguide with a sinusoidally rippled wall, producing very high-power coherent microwave radiation. A linear fluid model is used to study the effects of a dielectric liner in the device. The dispersion relation is derived and then solved numerically. It is found that, in the dielectric-lined sinusoidally rippled-wall cylindrical waveguide, the wave modes can be excited either in the backward-wave case or in the traveling-wave case, and the presence of the dielectric slows the normal modes of the structure, making it easier to achieve traveling-wave tube operation. Numerical results show that a rapid increase in the growth rate occurs when the dielectric constant reaches an optimum value, where a high-frequency mode may possess the largest peak growth rate provided other parameters are reasonably chosen. Therefore, one would expect the device to operate in the high-frequency regime with a much larger growth rate. However, in the limit of no dielectric liner, the results reduce to the regular ones, which show that the growth rate of the fundamental mode is the largest. In addition, if all of the beam parameters remain the same, the dielectric liner enhances the space-charge-limited current of the electron beam, which may also be beneficial for the generation of high-power microwave radiation.

PACS number(s): 52.75.Ms, 84.40.Fe, 41.60.Cr, 41.75.Ht

I. INTRODUCTION

Backward-wave tubes (BWT's) and traveling-wave tubes (TWT's) are successful examples of utilizing relativistic electron beams (REB's) which pass through slow-wave structures to generate high-power coherent microwave radiation. Many authors [1–10] have focused their attention on these devices for more efficient operation at high-power levels, and important results have been obtained both experimentally and theoretically. In recent years, several ideas have also been considered for enhancing the operating efficiency of the device, such as traveling-wave free-electron lasers [11], Cerenkov traveling-wave tubes with spatially varying dielectric constants [12], and BWT's using nonuniform slow-wave structures [13,14]. The introduction of a background plasma into the BWT or TWT is another proposal for improving the performance of the device. Experimental and theoretical results [15–17] have demonstrated that the background plasma enhances the operating efficiency of the BWT dramatically.

In this paper, we are motivated to present the concept of a dielectric BWT or TWT, where the slow-wave structure is a dielectric-lined rippled-wall cylindrical waveguide. This suggestion has an obvious advantage that, for a certain REB, the presence of a dielectric liner in the waveguide can partially neutralize the space-charge effects of the REB, and therefore increase the space-charge-limited current of the REB [18], which is profitable for the generation of high-power microwave radiation.

In fact, solving the Poisson equation, one can easily find that the space-charge-limited current for a dielectric-lined waveguide is approximately given by

$$I_{\mathrm{DL}}=\frac{(\gamma_0^{2/3}-1)^{3/2}mc^3/e}{1-\dfrac{2r_1^2}{r_2^2-r_1^2}\ln\dfrac{r_2}{r_1}+2\ln\dfrac{R_0}{r_2}+2\left[\dfrac{1-\varepsilon}{\varepsilon}\right]\ln\dfrac{R_0}{a}}, \tag{1}$$

where r_1 and r_2 are the inner radius and outer radius of an annular REB, respectively, R_0 is the waveguide radius, $a\,(a\geq r_2)$ is the inner radius of the dielectric-liner, ε is the dielectric constant, $-e$ and m are the electron charge and rest mass, respectively, $\gamma_0=(1-v_0^2/c^2)^{-1/2}$ is the relativistic factor of the REB, v_0 denotes the REB velocity, and c represents the speed of light in vacuum. Note that the region $a<r<R_0$ is filled with the dielectric material, and that the waveguide wall at $r=R_0$ is a perfect grounded conductor. When $\varepsilon=1$, Eq. (1) reduces to

$$I_L=\frac{(\gamma_0^{2/3}-1)^{3/2}mc^3/e}{1-\dfrac{2r_1^2}{r_2^2-r_1^2}\ln\dfrac{r_2}{r_1}+2\ln\dfrac{R_0}{r_2}}, \tag{2}$$

which is the well-known result of space-charge-limited current in a vacuum drift tube [19,20]. The results for a solid REB can be easily obtained by using $r_1=0$ in Eqs. (1) and (2).

From Eqs. (1) and (2), one can find that I_{DL} is larger than I_L when $\varepsilon>1$, and I_{DL}/I_L increases considerably with increasing the dielectric constant or the thickness of the dielectric liner. For example, I_{DL}/I_L will be as high as 3.0 for parameters $r_1/R_0=0.37$, $r_2/R_0=0.40$, $a/R_0=0.5$ and $\varepsilon=10.0$. Similarly, the addition of a dielectric liner in a rippled-wall waveguide also allows the propagation of the beam current which could be higher

than the vacuum space-charge limit for the same values of electron beam inner and outer radii, and waveguide radius.

In addition, the BWT and TWT are essentially different. In a BWT, the excited wave, having a negative group velocity, propagates opposite to the REB, whereas the TWT operates with a excited wave of positive group velocity, traveling parallel to the REB. However, in the dielectric-lined cylindrical waveguide with a sinusoidally rippled wall, the wave modes can be excited either in the backward-wave case or in the traveling-wave case. The addition of the dielectric slows the normal modes of the structure, making it easier to achieve TWT operation.

In order to understand the elementary physics of the dielectric BWT or TWT, we have developed a linear fluid model to derive the dispersion relation, and analyzed numerically the instability in the device. Our results reveal that the growth rate of the device may have a rapid increase when the dielectric constant reaches an optimum value, and that the device is expected to operate in the high-frequency regime with a much larger growth rate.

The remainder of this paper is as follows. In Sec. II we derive the dispersion relation of a BWT or TWT with a dielectric-lined sinusoidally rippled-wall cylindrical waveguide using a linear fluid model, in which the REB is guided by an infinitely strong axial magnetic field. In Sec. III we present the numerical results of the model. Conclusions are stated in Sec. IV.

II. DISPERSION RELATION

Consider a dielectric-lined rippled-wall cylindrical waveguide whose wall radius $R(z)$ varies sinusoidally according to the relation

$$R(z)=R_0+h\cos(k_0 z)\ , \tag{3}$$

where h is the ripple amplitude, $k_0=2\pi/z_0$ is the ripple wave number, z_0 denotes the ripple period, and R_0 represents the average radius of the waveguide. As shown in Fig. 1, a solid REB injects into the waveguide with velocity $\mathbf{v}_0=v_0\hat{z}$, radius r_b, and density n_0. The electrons in the beam are radially confined by an infinitely strong, externally applied magnetic field, and the region $a<r<R_1=R_0-h$ is filled with a dielectric material. In addition, we assume that there is no gap between the electron beam and the dielectric liner, say $r_b=a$, and that the system is azimuthally symmetric. It is further assumed that the waveguide wall is a perfect conductor, and that the waveguide is infinitely long.

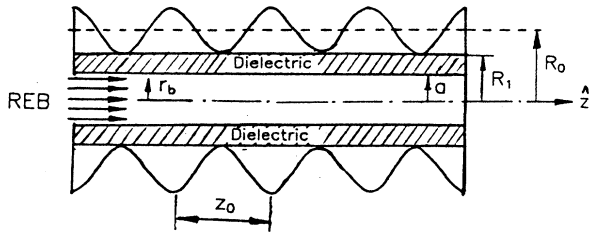

FIG. 1. A schematic picture of the device. A solid REB passes through a dielectric-lined cylindrical waveguide with a sinusoidally rippled wall. The system is immersed in an infinitely strong guide magnetic field.

Because of the infinite guide magnetic field, the transverse motion of the electrons is negligible, and the linear instability only excites axisymmetric TM modes in the system, which can axially bunch the electron beam. The periodicity of the slow-wave structure permits the field components of TM modes and the beam perturbations to be expanded in a series according to the Floquet theorem [21]. Following the method used by Swegle in Ref. [10], and Minami *et al.* in Ref. [17], one can solve the motion, continuity, and Maxwell equations for the beam-waveguide interaction, giving the following expressions of the axial and radial electric fields E_z and E_r for the axisymmetric TM electromagnetic modes:

$$E_z=\begin{cases}\displaystyle\sum_{n=-\infty}^{\infty}\Delta_n^1\Delta_n^2E_n^0J_0(p_{\perp n}r)\exp[i(k_nz-\omega t], & 0\le r\le r_b\\ \displaystyle\sum_{n=-\infty}^{\infty}\Delta_n^2E_n^0H_0(k_{\perp n}r)\exp[i(k_nz-\omega t)], & r_b\le r\le R_1\\ \displaystyle\sum_{n=-\infty}^{\infty}E_n^0G_0(\alpha_{\perp n}r)\exp[i(k_nz-\omega t)], & R_1\le r\le R(z)\ ,\end{cases} \tag{4}$$

$$E_r=\begin{cases}\displaystyle\sum_{n=-\infty}^{\infty}(-i)\frac{\Delta_n^1\Delta_n^2E_n^0k_np_{\perp n}}{\alpha_{\perp n}^2}J_1(p_{\perp n}r)\exp[i(k_nz-\omega t)], & 0\le r\le r_b\\ \displaystyle\sum_{n=-\infty}^{\infty}(-i)\frac{\Delta_n^2E_n^0k_n}{k_{\perp n}}H_1(k_{\perp n}r)\exp[i(k_nz-\omega t)], & r_b\le r\le R_1\\ \displaystyle\sum_{n=-\infty}^{\infty}(-i)\frac{E_n^0k_n}{\alpha_{\perp n}}G_1(\alpha_{\perp n}r)\exp[i(k_nz-\omega t)], & R_1\le r\le R(z)\ ,\end{cases} \tag{5}$$

where

$$p_{\perp n}^2=\left[\frac{\omega^2}{c^2}-k_n^2\right]\left[1-\frac{\omega_{pb}^2}{\gamma_0^3(\omega-k_n v_0)^2}\right], \tag{6}$$

$$k_{\perp n}^2=\frac{\varepsilon\omega^2}{c^2}-k_n^2, \tag{7}$$

$$\alpha_{\perp n}^2=\frac{\omega^2}{c^2}-k_n^2, \tag{8}$$

$$k_n=nk_0+k_z, \tag{9}$$

$$\omega_{pb}=\left[\frac{4\pi e^2 n_0}{m}\right]^{1/2}, \tag{10}$$

$$H_0(k_{\perp n}r)=K_nJ_0(k_{\perp n}r)+L_nN_0(k_{\perp n}r), \tag{11}$$

$$H_1(k_{\perp n}r)=K_nJ_1(k_{\perp n}r)+L_nN_1(k_{\perp n}r), \tag{12}$$

$$G_0(\alpha_{\perp n}r)=P_nJ_0(\alpha_{\perp n}r)+Q_nN_0(\alpha_{\perp n}r), \tag{13}$$

$$G_1(\alpha_{\perp n}r)=P_nJ_1(\alpha_{\perp n}r)+Q_nN_1(\alpha_{\perp n}r), \tag{14}$$

$$\Delta_n^1=J_0(k_{\perp n}r_b)N_1(k_{\perp n}r_b)-J_1(k_{\perp n}r_b)N_0(k_{\perp n}r_b), \tag{15}$$

$$\Delta_n^2=J_0(\alpha_{\perp n}R_1)N_1(\alpha_{\perp n}R_1)-J_1(\alpha_{\perp n}R_1)N_0(\alpha_{\perp n}R_1), \tag{16}$$

$$K_n=J_0(p_{\perp n}r_b)N_1(k_{\perp n}r_b)-\frac{p_{\perp n}k_{\perp n}}{\varepsilon\alpha_{\perp n}^2}J_1(p_{\perp n}r_b)N_0(k_{\perp n}r_b), \tag{17}$$

$$L_n=\frac{p_{\perp n}k_{\perp n}}{\varepsilon\alpha_{\perp n}^2}J_0(k_{\perp n}r_b)J_1(p_{\perp n}r_b)-J_0(p_{\perp n}r_b)J_1(k_{\perp n}r_b), \tag{18}$$

$$P_n=K_n\left[J_0(k_{\perp n}R_1)N_1(\alpha_{\perp n}R_1)-\frac{\varepsilon\alpha_{\perp n}}{k_{\perp n}}J_1(k_{\perp n}R_1)N_0(\alpha_{\perp n}R_1)\right]+L_n\left[N_0(k_{\perp n}R_1)N_1(\alpha_{\perp n}R_1)-\frac{\varepsilon\alpha_{\perp n}}{k_{\perp n}}N_1(k_{\perp n}R_1)N_0(\alpha_{\perp n}R_1)\right], \tag{19}$$

$$Q_n=K_n\left[\frac{\varepsilon\alpha_{\perp n}}{k_{\perp n}}J_1(k_{\perp n}R_1)J_0(\alpha_{\perp n}R_1)-J_0(k_{\perp n}R_1)J_1(\alpha_{\perp n}R_1)\right]+L_n\left[\frac{\varepsilon\alpha_{\perp n}}{k_{\perp n}}N_1(k_{\perp n}R_1)J_0(\alpha_{\perp n}R_1)-N_0(k_{\perp n}R_1)J_1(\alpha_{\perp n}R_1)\right]. \tag{20}$$

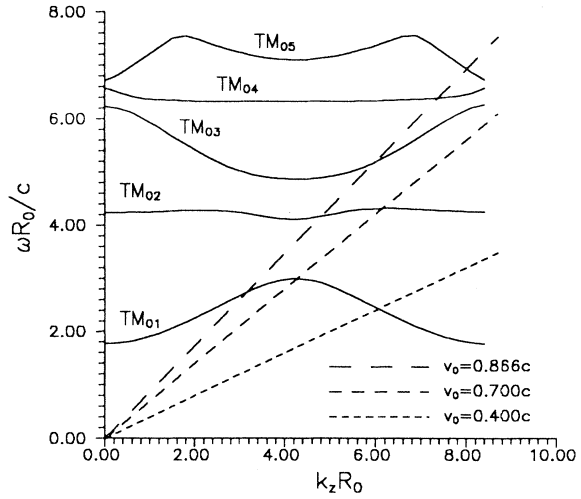

FIG. 2. Numerical solution of the uncoupled dispersion relation for $k_0R_0=8.5$, $a/R_0=0.3$, $h/R_0=0.2$, $\epsilon=2.25$, and $\omega_{pb}R_0/c=0$.

Also, J_n and N_n are the Bessel functions of order n of the first and second kinds, ω and k_z are the angular frequency and longitudinal wave number of the TM mode, E_n^0 is the amplitude of the nth harmonic component of the electric field, ε is the dielectric constant, $\gamma_0=(1-v_0^2/c^2)^{-1/2}$ is the relativistic factor of the REB, $-e$ and m are the electron charge and rest mass, and c represents the speed of light in vacuum. It may be mentioned that, in deriving the expressions of $E_z(r)$ and $E_r(r)$, the boundary conditions that $E_z(r)$ and $D_r(r)=\varepsilon E_r(r)$ are continuous across the interface between the beam and dielectric regions are employed.

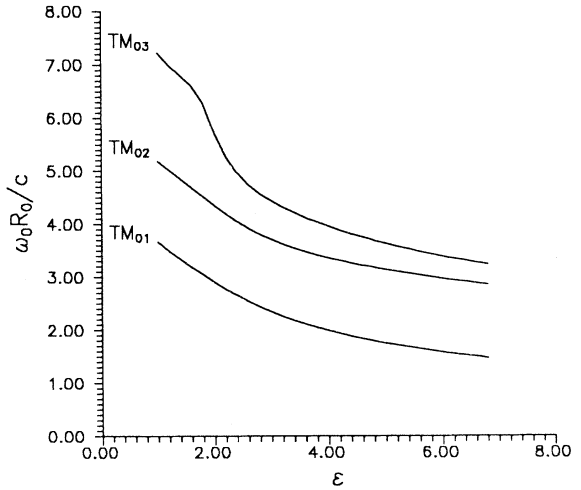

FIG. 3. The eigenfrequencies of the three lowest modes TM_{01}, TM_{02}, and TM_{03} vs the dielectric constant ε for $k_0R_0=8.5$, $a/R_0=0.3$, $h/R_0=0.2$, and $\gamma_0=2.0$.

Because the tangential electric field E_t must be zero at the perfectly conducting rippled-wall waveguide surface, E_z and E_r must satisfy the following condition:

$$E_z(r=R(z))+E_r(r=R(z))dR/dz=0 . \quad (21)$$

Substituting (4) and (5) into (21), multiplying (21) by $\exp[-imk_0z]$, and integrating from $z=-\pi/k_0$ to $z=\pi/k_0$, one can obtain

$$\overleftrightarrow{D}\cdot\vec{A}=0 , \quad (22)$$

where $\vec{A}$ is a column vector with elements $A_n=E_n^0$, and $\overleftrightarrow{D}$ is a matrix with elements

$$D_{mn}=\int_{-\pi/k_0}^{\pi/k_0} dz \left\{ G_0(\alpha_{\perp n}R(z))+\frac{ik_nk_0h}{\alpha_{\perp n}}\sin(k_0z)G_1(\alpha_{\perp n}R(z)) \right\} e^{i(n-m)k_0z} . \quad (23)$$

The dispersion relation for the device is then expressed by the determinant equation

$$\det[\overleftrightarrow{D}]=0 . \quad (24)$$

When no beam is present ($\omega_{pb}=0$), Eq. (24) can be used to study the uncoupled modes of the dielectric-lined rippled-wall waveguide. It is difficult to give analytical solutions of Eq. (24), so we will solve Eq. (24) by the numerical method. It is noticed that the present paper calculates elements D_{mn} of Eq. (23) directly using an efficient computer code, differing from the model of Ref. [17] in which the elements D_{mn} for the case of a plasma-filled BWT are Taylor expanded around $R(z)=R_0$.

III. NUMERICAL RESULTS

Although $\overleftrightarrow{D}$ is an infinite matrix, in practice we must truncate $\overleftrightarrow{D}$ to some manageable size [10]. Typically, we use a 5×5 matrix with $-2\le m,n\le2$, because we have carried out the numerical calculations of 7×7 matrices and obtained essentially the same results for the parameters given in the examples involved.

The uncoupled dispersion relation is shown in Fig. 2, where we have plotted $\omega R_0/c$ versus k_zR_0 for $k_0R_0=8.5$, $a/R_0=0.3$, $h/R_0=0.2$, $\varepsilon=2.25$, and $\omega_{pb}R_0/c=0$. The five lowest modes are labeled as TM_{01}, TM_{02}, TM_{03}, TM_{04}, and TM_{05} modes, respectively. Note that this labeling scheme is usually employed for smooth-walled waveguide modes. In fact, the TM mode structure in a rippled-wall waveguide differs from the TM mode structure in a smooth-walled waveguide. The labeling scheme used in the present paper is only for the sake of convenience. Here, as can be seen from Fig. 2, the angular frequency ω varies periodically with the wave number k_z, and the space-charge wave, indicated by a straight dashed line in the figure, interacts with the five modes, producing high-power microwave radiation. The intersections of the space-charge wave with the five modes are considered to be the eigenfrequencies of the device. It is worth noting that other high-frequency modes were not calculated for presentation in the present paper. We can see from Fig. 2 that the space-charge wave with a beam velocity of $v_0=0.4c$ intersects the TM_{01} mode at a point where the group velocity of the wave is negative, whereas the space-charge wave with a beam velocity of $v_0=0.866c$ intersects the TM_{01} mode at a point where the group velocity of the wave is positive. Therefore, the fundamental TM_{01} mode can be excited either in the backward-wave case or in the traveling-wave case. Obviously, the addition of the dielectric slows the normal modes of the structure, making it easier to achieve TWT operation. It may be mentioned that, in the limit of no dielectric liner, the wave modes may also be excited in both backward- and traveling-wave cases for a sinusoidally rippled-wall waveguide [10], but the ripple amplitude, ripple period, and beam energy must all be chosen reasonably.

Figure 3 gives the eigenfrequencies of the three lowest modes TM_{01}, TM_{02}, and TM_{03} versus the dielectric constant ε for $k_0R_0=8.5$, $a/R_0=0.3$, $h/R_0=0.2$, and $\gamma_0=0.2$. We can clearly see that the eigenfrequencies decrease monotonically as the dielectric constant ε increases. Therefore, the dielectric constant can be another tunable parameter for changing the operating frequency of the device.

To obtain the growth rates, one can solve Eq. (22) for complex roots of ω, assuming real values of k_z. For this purpose we must consider a nonzero value of ω_{pb}, which means the presence of a REB. The growth rate $\Gamma=\mathrm{Im}(\omega)$ indicates the interaction of the REB with the wave mode, providing information about the rise time of a microwave signal in an actual device.

In the case of no dielectric liner, the relation between the growth rate and the wave mode is shown in Fig. 4, where we have plotted the growth rates versus the wave number for $k_0R_0=8.5$, $r_b/R_0=0.3$, $h/R_0=0.2$, $\omega_{pb}R_0/c=0.2$, $\varepsilon=1.0$, and $\gamma_0=1.5$. It can be seen from Fig. 4 that each curve has a peak near $\omega\approx k_zv_0$, which represents a stronger beam-wave interaction. In addition, the higher-frequency mode possesses a lower growth rate, and the peak growth rate of the TM_{01} mode is the largest. In the case of a dielectric liner loaded in the device, the peak growth rate of each mode increases rapidly with the dielectric constant, and reaches a maximum value as the dielectric constant is near an optimum value, where some higher-frequency modes may possess larger growth rates. These are shown in Figs. 5 and 6, respectively. Figure 5 displays the peak growth rates of TM_{01}, TM_{02}, and TM_{03} modes versus the dielectric constant for $k_0R_0=8.5$, $a/R_0=0.3$, $h/R_0=0.2$, $\omega_{pb}R_0/c=0.2$, and

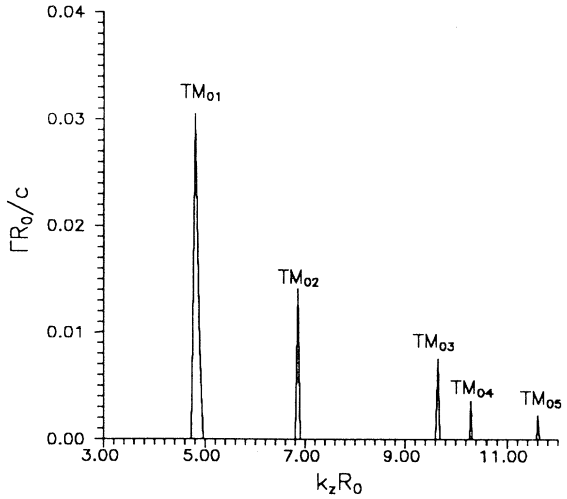

FIG. 4. The growth rates vs the wave number in the case of no dielectric liner for $k_0R_0=8.5$, $r_b/R_0=0.3$, $h/R_0=0.2$, $\omega_{pb}R_0/c=0.2$, $\varepsilon=1.0$, and $\gamma_0=1.5$.

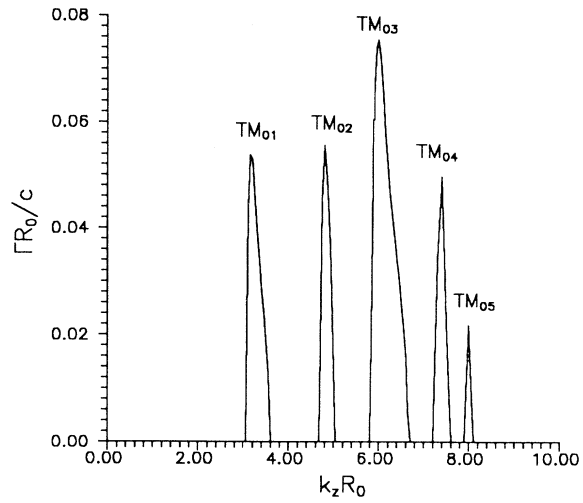

FIG. 6. The growth rates of TM_{01}, TM_{02}, TM_{03}, TM_{04}, and TM_{05} modes vs the wave number in the presence of a dielectric liner for $k_0R_0=8.5$, $a/R_0=0.3$, $h/R_0=0.2$, $\omega_{pb}R_0/c=0.2$, $\varepsilon=2.25$, and $\gamma_0=2.0$.

$\gamma_0=2.0$. Figure 6 illustrates the growth rates of TM_{01}, TM_{02}, TM_{03}, TM_{04}, and TM_{05} modes versus the wave number for $k_0R_0=8.5$, $a/R_0=0.3$, $h/R_0=0.2$, $\omega_{pb}R_0/c=0.2$, $\varepsilon=2.25$, and $\gamma_0=2.0$. As can be seen from Figs. 5 and 6, the high-frequency mode TM_{03} may possess the largest peak growth rate as long as a reasonable value of dielectric constant is chosen. Hence one would expect the device to operate in the high-frequency regime with a much larger growth rate. In addition, it is worth noting that, as shown in Fig. 5, a very high dielectric constant may reduce the growth rate considerably, which is unprofitable for the microwave instability.

To understand the numerical results of the present paper, one can refer to the approximate scalings of Ref. [7]. As shown in Ref. [7], the peak growth rate of a BWT or TWT is $\Gamma_{\max}\propto\Delta^{1/3}$, where Δ is $O[(h/R_0)^{2|n|}]$ for a small value of h/R_0, and n represents the nth Hartree harmonic interacting resonantly with the beam mode $\omega=k_zv_0$. Thus the peak growth rate decreases with increasing $|n|$. This conclusion also applies to the situation of the present paper, although the value of h/R_0 is relatively larger [7]. Figure 7 shows $\omega R_0/c$ versus k_zR_0 for $k_0R_0=8.5$, $r_b/R_0=0.3$, $h/R_0=0.2$, $\gamma_0=1.5$, $\varepsilon=1.0$, and $\omega_{pb}R_0/c=0$, giving the uncoupled dispersion relation of no dielectric. Following the method used in Ref.

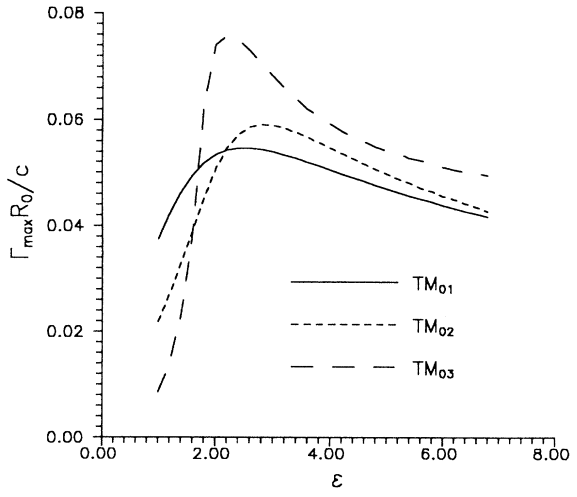

FIG. 5. The peak growth rates of TM_{01}, TM_{02}, and TM_{03} modes vs the dielectric constant ε for $k_0R_0=8.5$, $a/R_0=0.3$, $h/R_0=0.2$, $\omega_{pb}R_0/c=0.2$, and $\gamma_0=2.0$.

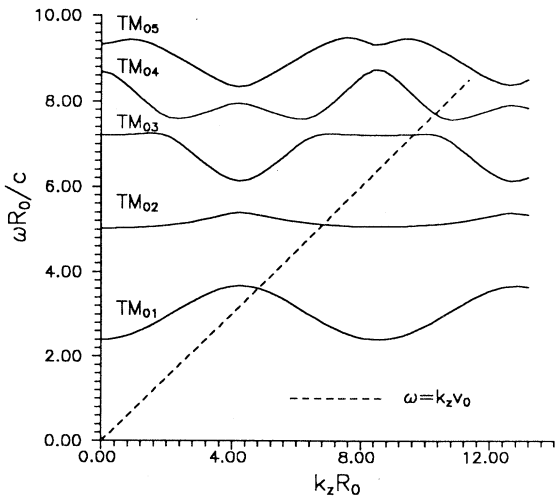

FIG. 7. Numerical solution of the uncoupled dispersion relation in the case of no dielectric liner for $k_0R_0=8.5$, $r_b/R_0=0.3$, $h/R_0=0.2$, $\gamma_0=1.5$, $\varepsilon=1.0$, and $\omega_{pb}R_0/c=0$.

[7], one can determine from Fig. 7 that the TM_{01} and TM_{02} modes are excited in the regime where the electron beam interacts mainly with the first Hartree harmonic ($n=-1$), whereas the TM_{03} mode is excited in the regime where the second Hartree harmonic ($n=-2$) may take effect. Obviously, the peak growth rate of the TM_{03} mode is lower than those of TM_{01} and TM_{02} modes. In order to compare the growth rates of TM_{01} and TM_{02} modes, we can display the longitudinal electric fields of the first Hartree harmonic for TM_{01} and TM_{02} modes since the electric fields are comparable for the same order Hartree harmonic. The strength of the longitudinal electric field is one of the major factors that can affect the growth rate of the device. It is seen that Eq. (22) can be solved for all of the E_n^0's but one, so we can then choose, for example, $C_n=\Delta_n^1\Delta_n^2E_n^0=1$ for $n=-1$. The normalized longitudinal electric fields $E_{z,n}/C_n$ of the first Hartree harmonic ($n=-1$) for TM_{01} and TM_{02} modes are shown in Fig. 8, where we have plotted $E_{z,-1}/C_{-1}$ versus r/R_0 for $k_0R_0=8.5$, $r_b/R_0=0.3$, $h/R_0=0.2$, $\gamma_0=1.5$, and $\varepsilon=1.0$. It can be seen that, in the interaction region ($0\le r/R_0\le r_b/R_0$), the first Hartree harmonic field for the TM_{01} mode is stronger than that for the TM_{02} mode. Therefore, in the case of no dielectric liner, the peak growth rate of the TM_{01} mode is higher than those of TM_{02} and TM_{03} modes for the parameters involved in Fig. 4. Further, the peak growth rate of the TM_{01} mode may be the highest, because other high-frequency modes, like TM_{04} and TM_{05}, are excited in the regime where the REB interacts mainly with the higher-order Hartree harmonics ($n<-1$).

The results are quite different in the case of a dielectric liner loaded in the device, in which some higher-order modes may have larger growth rates. Physically, when adding a dielectric liner in the waveguide, the dielectric allows the mode to be well located within the interaction region $0\le r\le a$, making the mode possess a lower phase

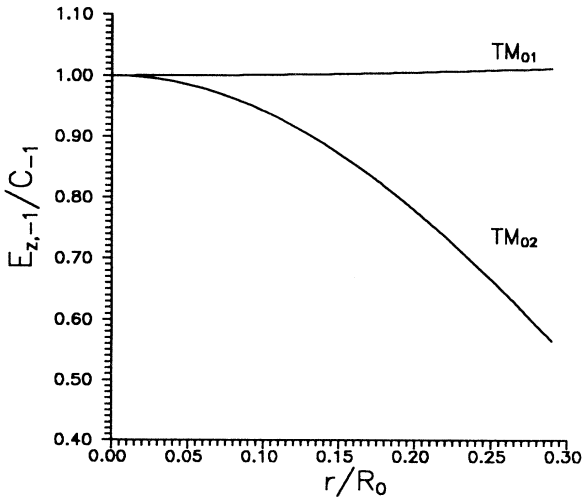

FIG. 8. The normalized longitudinal electric fields of the first Hartree harmonic ($n=-1$) for TM_{01} and TM_{02} modes vs r/R_0 in the case of no dielectric liner when $k_0R_0=8.5$, $r_b/R_0=0.3$, $h/R_0=0.2$, $\gamma_0=1.5$, and $\varepsilon=1.0$.

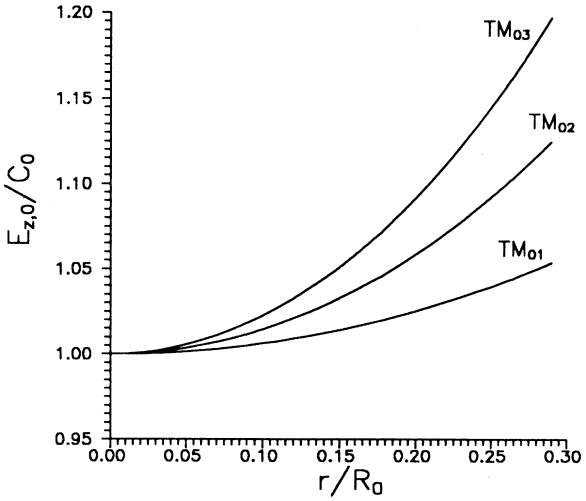

FIG. 9. The normalized longitudinal electric fields of zero-order Hartree harmonic ($n=0$) for TM_{01}, TM_{02}, and TM_{03} modes vs r/R_0 in the presence of a dielectric liner when $k_0R_0=8.5$, $a/R_0=0.3$, $h/R_0=0.2$, $\gamma_0=2.0$, and $\varepsilon=2.25$.

velocity. In this case, the electric field in the interaction region is stronger, and the growth rate is larger. Particularly, for the parameters of Fig. 6, we can see from Fig. 2 that the TM_{01}, TM_{02}, and TM_{03} modes are excited in the regime where the electron beam (with $v_0/c=0.866$) interacts mainly with the zero-order Hartree harmonic. In order to compare the peak growth rates of TM_{01}, TM_{02}, and TM_{03} modes, it is also necessary to display the normalized electric fields $E_{z,n}/C_n$ of the zero-order Hartree harmonic ($n=0$) for TM_{01}, TM_{02}, and TM_{03} modes. Figure 9 shows $E_{z,0}/C_0$ versus r/R_0 for $k_0R_0=8.5$, $a/R_0=0.3$, $h/R_0=0.2$, $\gamma_0=2.0$, and $\varepsilon=2.25$. We can see that, in the interaction region, the zero-order Hartree harmonic field for TM_{03} mode is the strongest, and therefore the peak growth rate of the TM_{03} mode is larger than those of TM_{01} and TM_{02} modes. This analysis may explain the conclusion that the growth rates are larger for some higher-order modes in the presence of a dielectric. However, it may be mentioned that much higher-order modes, like TM_{04} and TM_{05}, are excited in the regime where higher-order Hartree harmonics ($n\le -1$) could take effect, and, consequently, their growth rates may be decreased.

IV. CONCLUSIONS

We have developed a linear theory to study the concept of a dielectric BWT or TWT, in which the slow-wave structure is a dielectric-lined rippled-wall cylindrical waveguide immersed in an infinitely large axial magnetic field. The dispersion relation is analyzed numerically, and the effects of the dielectric liner in the device are also explored. The validity of the analysis depends on the requirement that the length of the structure be significantly longer than its mean radius. It is found that

the presence of a dielectric liner in the sinusoidally rippled-wall waveguide may modify the wave mode structures favorably, and improve the beam-waveguide interaction as long as a reasonable value of dielectric constant is chosen. Growth rates are observed to increase as the dielectric constant is made larger, and peak at optimum values of the dielectric constant, where some high-frequency modes may have much larger growth rates and the growth rate of the TM_{03} mode may be the largest. This is in contrast to the case of no dielectric liner, in which the fundamental TM_{01} mode possesses the largest growth rate.

In the absence of the dielectric liner, the excitation of traveling-wave TM_{01} mode depends closely on the ripple amplitude, ripple period, and REB energy. However, the addition of the dielectric slows the normal modes of the structure, making it easier to achieve TWT operation. Additionally, if all of the beam parameters remain the same, the dielectric liner can enhance the space-charge-limited current of the REB obviously. The enhancement of the limited current is profitable for the generation of microwave radiation, because devices using REB's to generate coherent microwaves usually require larger current propagation in the tube for power enhancement.

In conclusion, the BWT or TWT studied in the present paper can be expected to operate in the high-frequency regime with a much larger growth rate. Although the dielectric liner leads to a decrease in the operating frequency of the device, the system, as mentioned above, may excite a high-frequency mode having the largest growth rate. Finally, it is important to note that a nonlinear theory is needed to determine the saturation efficiency of this device, and more detailed studies should be done.

[1] Y. Carmel, J. Ivers, R. E. Kribel, and J. Nation, Phys. Rev. Lett. **33**, 1278 (1974).
[2] L. S. Bogdankevich, M. V. Kuzelev, and A. A. Rukhadze, Zh. Tekh. Fiz. **50**, 233 (1980) [Sov. Phys. Tech. Phys. **25**, 143 (1980)].
[3] Y. Carmel, V. L. Granatstein, and A. Gover, Phys. Rev. Lett. **51**, 566 (1983).
[4] R. A. Kehs, A. Bromborsky, B. G. Ruth, S. E. Graybill, W. W. Destler, Y. Carmel, and M. C. Wang, IEEE Trans. Plasma Sci. **PS-13**, 559 (1985).
[5] J. A. Swegle, Phys. Fluids **28**, 3696 (1985).
[6] Y. Carmel, K. Minami, R. A. Kehs, W. W. Destler, V. L. Granatstein, D. Abe, and W. L. Lou, Phys. Rev. Lett. **62**, 2389 (1989).
[7] J. A. Swegle, Phys. Fluids **30**, 1201 (1987).
[8] L.S. Bogdankevich, M. V. Kuzelev, and A.A. Rukhadze, Usp. Fiz. Nauk. **133**, 3 (1981) [Sov. Phys. Usp. **24**, 1 (1981)].
[9] L. Earley, G. T. Leifeste, R. B. Miller, J.W. Poukey, J. A. Swegle, and C. Christ, Bull. Am. Phys. Soc. **29**, 1292 (1984).
[10] J. A. Swegle, J. W. Poukey, and G. T. Leifeste, Phys. Fluids **28**, 2882 (1985).
[11] E. Jerby, Phys. Rev. A **44**, 703 (1991).
[12] L. Schachter, Phys. Rev. A **43**, 3785 (1991).
[13] S. D. Korovin, S. D. Polevin, A. M. Roitman, and V. V. Rostov, Pis'ma Zh. Tekh. Fiz. **18**, 63 (1992) [Sov. Tech. Phys. Lett. **18**, 265 (1992)].
[14] L. D. Moreland, E. Schamiloglu, R.W. Lemke, S. D. Korovin, V. V. Rostov, A. M. Roitman, K. J. Hendricks, and T. A. Spencer, IEEE Trans. Plasma Sci. **PS-22**, 554 (1994).
[15] Y. Carmel, W. R. Lou, T. M. Antonsen, Jr., J. Rodgers, B. Levush, W. W. Destler, and V. L. Granatstein, Phys. Fluids B **4**, 2286 (1992).
[16] D. M. Goebel, J. M. Butler, R. W. Schumacher, J. Santoru, and R. L. Eisenhart, IEEE Trans. Plasma Sci. **PS-22**, 547 (1994).
[17] K. Minami, Y. Carmel, V. L. Granatstein, W. W. Destler, W. Lou, D. K. Abe, R.A. Kehs, M. M. Ali, T. Hosokawa, K. Ogura, and T. Watanabe, IEEE Trans. Plasma Sci. **PS-18**, 537 (1990).
[18] Bao-Liang Qian, Yong-Gui Liu, and Chuan-Lu Li (unpublished).
[19] L. S. Bogdankevich and A. A. Rukhadze, Usp. Fiz. Nauk. **103**, 609 (1971) [Sov. Phys. Usp. **14**, 163 (1971)].
[20] R. B. Miller and D. C. Straw, J. Appl. Phys. **47**, 1897 (1976).
[21] C. C. Johnson, *Field and Wave Electrodynamics* (McGraw-Hill, New York, 1965).